Composites Part C: Open Access 15 (2024) 100524

Contents lists available at ScienceDirect

Composites Part C: Open Access

journal homepage: www.sciencedirect.com/journal/composites-part-c-open-access

A machine learning enhanced characteristic length method for failure prediction of open hole tension composites

Omar A.I. Azeem *, Silvestre T. Pinho

Department of Aeronautics, Imperial College London, Exhibition Road, London SW7 2AZ, UK

ARTICLE INFO

Keywords:
Machine learning
Characteristic length method
Open holes

ABSTRACT

The characteristic length method is a non-local approach to predicting the failure of open and closed-hole composite features. This method requires the determination of the linear elastic stress field of the composite laminate at its failure load. Typically, this requires computationally expensive progressive damage and linear elastic modelling and simulation with finite element analysis (FEA). In this study, we demonstrate the benefit of machine learning methods to efficiently and accurately predict characteristic lengths of composite laminates with open holes. We find that the prediction of the load-displacement profile usefully informs ultimate failure load prediction. We also find that linear elastic stress fields are more accurately predicted using a long-short term memory neural network rather than a convolutional decoder neural network. We show indirect prediction of characteristic length, via prediction of failure loads and linear elastic stress fields independently, results in more flexible, interpretable and accurate results than direct prediction of characteristic length, given sufficient training data. Our machine learning-assisted characteristic length method shows over five orders of magnitude of time-saving benefit compared to FEA-based methods.

1. Introduction and literature review

1.1. Characteristic length method

Holes exist in composite structures, for instance for lightening purposes and access purposes. Bolted joints remain commonplace in composite structures, and as a result fastener holes [1]. It is important to predict hole failure quickly and accurately for sizing and optimisation operations in the design stage of composite structures. The characteristic length method is a commonly used approach for failure prediction during the design stage, that accounts for notch sensitivity and the hole size effect [2,3]. The overall workflow for the characteristic length method is depicted in Fig. 1.

The linear elastic stress distribution in the net section plane (perpendicular to loading) at its failure load is determined for a coupon specimen with an open hole. The characteristic length is determined as the distance from the hole boundary at which the stress is equal to a critical stress (point stress criterion). Alternatively, it is defined by the distance over which average stress is equal to the critical stress (average stress criterion) [2]. This critical stress can be the unnotched failure stress, notched failure stress, or a combination of stresses that interact to cause failure under a failure criterion. Yamada Sun failure criterion is commonly used, as hole failure is typically driven by fibre kinking [4,5]. For closed holes, the same operations are done in the bearing plane (parallel to loading), and a characteristic curve is derived by elliptically joining characteristic lengths in the bearing and bypass (net section) planes [6]. This characteristic distance can be used to predict the failure of in-situ open holes in linear elastic composite structural models.

Linear elastic stress distributions require finite element analyses, or the use of semi-analytical solutions based on the Lekhnitskii formalism [7,8], for example. In efforts to reduce the experimental campaign to derive failure loads, modifications to this characteristic length method include using progressive damage modelling [5], an analytical method to determine characteristic distance [9], and curve fitting methods to predict characteristic distance given varying geometric parameters [10]. Furthermore, alternative methods to characteristic length methods include those based on cohesive zone modelling [11], inherent flaw modelling based on linear elastic fracture mechanics [12], and methods based on finite fracture mechanics [13,14,15].

* Corresponding author.
E-mail address: oai15@imperial.ac.uk (O.A.I. Azeem).

https://doi.org/10.1016/j.jcomc.2024.100524

Available online 10 October 2024

1.2. Machine learning for stress analysis and failure loads

In this study, however, we aim to use machine learning to eliminate the online FE modelling and simulation as required by the characteristic length method. FE is instead used to train our machine learning models offline, saving the stress analyst time during the predictive virtual testing process. Direct prediction of characteristic length has been done in a previous study for varying geometric parameters [10]. However, direct prediction results in highly black box predictions, making it difficult to diagnose whether errors in characteristic length prediction are due to erroneous stress fields or failure loads. Breaking up a highly non-linear problem, into multiple problems that are each more linear, should allow for less black-box modelling and improved prediction performance. Furthermore, direct prediction requires that a certain failure criterion is encoded in the training data to determine the characteristic length. Therefore, direct prediction is less flexible to changes in selected failure criterion.

In this study, we wish to produce a transparent and flexible workflow. Therefore, we aim to use machine learning to predict the stress decay of the linear models in the net section planes in a computationally efficient manner. Furthermore, we aim to use machine learning to predict the failure load of notched coupon specimens in a computationally efficient manner. These machine learning-assisted predictions will therefore allow fast and easy determination of characteristic lengths.

Machine learning has been used in combination with high-fidelity finite element analysis for structural health modelling and fatigue performance prediction [16,17]. Machine learning has previously been used for linear elastic stress analysis in composite structures [18,19,20]. Typically, image-based neural networks, such as convolutional neural networks, U-nets and generative adversarial neural networks have been used to predict stress fields. In previous work, we used an analytical solution-informed U-net to predict the stress field in the net section plane of notched composites in a multi-fidelity framework [21]. However, the convolutional filters used in this study led to irregular stress distribution predictions. We have also used sequential neural networks to predict through-thickness stress distributions of volume-averaged stresses for notched composites in a multi-fidelity framework [22]. However, the accuracy of sequential neural networks to predict point stresses across the net section plane remains to be determined. Therefore, in this study, we compare the use of sequential neural networks and convolutional neural networks to predict the stress field in the net section plane.

Machine learning has previously been used to predict failure loads of composites structures [23,24]. Random Forest, XGBoost, Gaussian Process Regression and Artificial Neural Networks (ANNs) have been used to predict the tensile strength of notched composites as a surrogate for an analytical solution [15]. However, such methods have not been used following progressive damage modelling to predict tensile strength. Therefore, in this study, we use these shallow neural networks to directly predict the failure load derived by progressive damage models.

In another study, a probabilistic neural network trained on experimental results is used to predict the probability of failure. Following this, a bi-section search method is used to indirectly determine the tensile strength that results in a high likelihood of failure [25]. A currently unexplored idea is to predict failure load indirectly by extracting the maximum of a predicted load-displacement profile. It is hypothesized that prediction of the load-displacement profile allows contextual information, such as stiffness and failure strain, that enables better maximum load prediction.

Machine learning has been used to predict stress-strain and load-displacement profiles [26,27,28]. Artificial neural networks and sequential neural networks lend themselves to such use. In this study, we use artificial neural networks to indirectly predict maximum failure load via prediction of the load-displacement profile. This will be compared to the direct prediction of failure load with artificial neural networks.

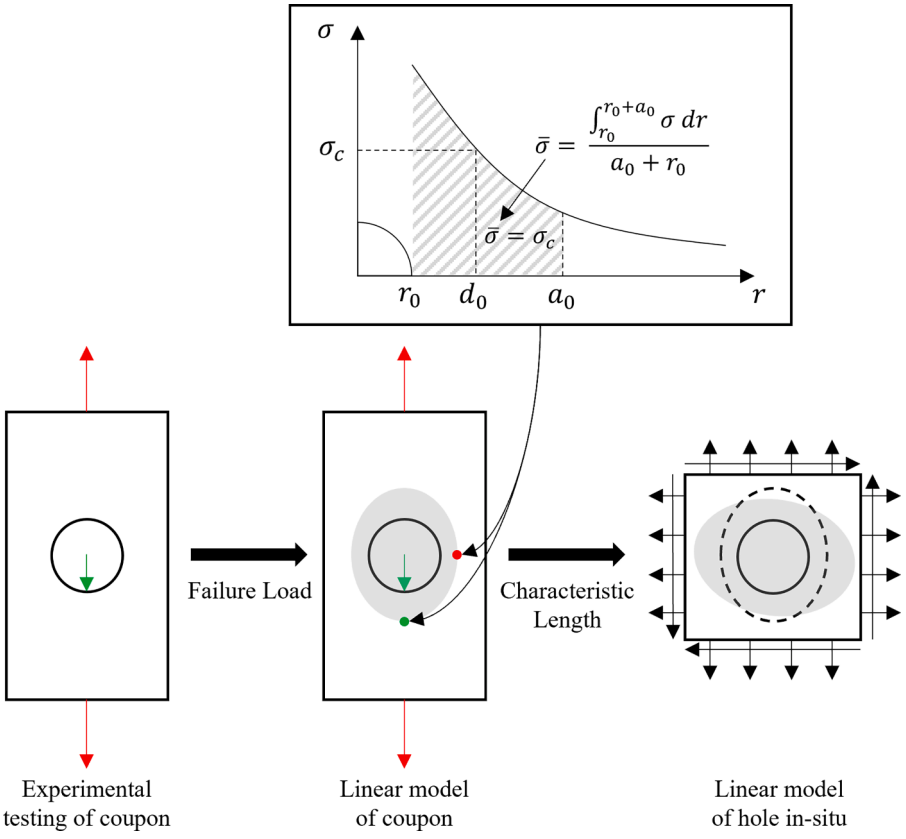

Fig. 1. Characteristic length method.

1.3. Aims and objectives

In the context of an open-hole composite laminate, the complete objectives of this study are to:

- Predict the maximum load directly using various neural networks.
- Predict the maximum load indirectly from the prediction of the load-displacement profile using an artificial neural network.
- Predict the linear elastic stress distributions in the net section plane, comparing the use of sequential neural networks and convolutional neural networks.
- Predict the characteristic length indirectly via the prediction of failure load and linear elastic stress distributions and compare them with the direct prediction of characteristic length.

2. Methodology

2.1. Workflow

To train our machine learning models, we generate linear elastic and progressive damage models for open-hole coupon specimens of varying hole geometry and laminate stacking sequence. The design of experiment used in this study follows the methodology of previous work [22]. This design of experiment results in a well-distributed sampling of laminate stacking sequence in both the lamination parameters space and the ply angle space.

Python scripting is used to generate linear elastic and progressive damage finite element models in Abaqus [29]. The linear elastic model has a unit load applied. The progressive damage model is run up to and beyond ultimate failure. The load-development profile is extracted from the progressive damage simulations and saved to a CSV file. The stress field is re-interpolated into a mesh-independent format using Paraview [30]. This is performed by converting the odb file to a vtu file and using the 'CellDatatoPointData' and 'PlotOverLine' functions with a suitable sampling resolution. The stress field in the net section plane is then transformed into an image. The average stress field is scaled by the failure load, as determined by the maximum load of the load-development plot. Characteristic lengths are determined by the application of a Yamada Sun failure criterion [5] given by:

$$\textit{Failure index} = \begin{cases} \sqrt{\left(\frac{\sigma_{11}}{X_T}\right)^2 + \left(\frac{\sigma_{12}}{S_{is}}\right)^2} & (\sigma_{11} > 0) \\ \sqrt{\left(\frac{\sigma_{11}}{X_C}\right)^2 + \left(\frac{\sigma_{12}}{S_{is}}\right)^2} & (\sigma_{11} < 0) \end{cases} \quad (1)$$

where the stress components σ_{11} and σ_{12}, are compared to the tensile strength X_T, compressive strength X_C, and in-situ shear strength S_{is}. The Yamada Sun failure criterion is most commonly used for the characteristic length method [4,5]. These characteristic lengths are also saved to a CSV file.

Random Forest, XGBoost, Gaussian Process Regression and ANN are used to predict the maximum of the load-development plot directly. An ANN is also used to predict the load-development profile, and the maximum failure load is therefore predicted indirectly. Inputs are normalised for improved performance.

Bidirectional long short-term memory neural networks and convolutional U-net inspired neural networks are used to predict the stress field in the net section plane. The predicted stress field at the predicted failure load can then be used to determine the predicted characteristic distance. Outputs are standardised for improved performance.

2.2. Machine learning models

We use TensorFlow [31] and Keras [32] to develop our ML models. A short explanation of the models used in this study is given below. Grid searches are used to determine the hyperparameters of models.

Random forest makes ensembled predictions made by multiple decision trees [33]. Decision trees work by hierarchically defining simple decision rules to predict data. They can have target variables which are discrete as for classification problems, or continuous as for regression problems. However, they particularly suffer from issues such as overfitting, and therefore ensembling is required. Bootstrap aggregation, known as bagging, is the ensembling method used. By sampling with replacement for each decision tree, we can average their predictions to result in a final, more robust, prediction. We can also visualise decision trees and therefore they are more interpretable than other machine learning models.

XGBoost is a popular and successful version of random forest which uses gradient boosting as the ensembling method [34]. Here, decision trees are trained sequentially to minimise the error of the previous decision tree.

Gaussian processes are a form of Bayesian machine learning. Bayesian methods consider a prior distribution, which is updated with observed samples to result in a posterior distribution of functions. Prior and posterior (joint distributions) are assumed to follow Gaussian distributions, defined by mean and covariance vectors [35]. Knowledge of prior distributions can be encoded by consideration of the learning kernel used to maximise log marginal likelihood [36]. The generalisability and tailorability offered by this machine learning method have resulted in considerable success for problems with low training dataset size.

Artificial neural networks are the basis for deep neural networks which are finding success for highly non-linear problems. They consist of hidden layers that sequentially perform non-linear operations using a defined activation function on the output of the previous layer and a set of weight and biases [37]. The prediction error is minimised by back-propagation to result in a refined set of weights and biases, which can then be used on unseen data to make predictions [38].

Long-short term memory neural networks (LSTM) belong to the family of sequential artificial neural networks, which have found success in time-series forecasting. As opposed to traditional artificial neural networks, where inputs and outputs are considered independently, such networks consider input and output sequentially. In previous work, we used a modified version of LSTM to predict ply-by-ply stress values, see Fig. 2a [22]. These modifications include reformulation of the LSTM from a time-basis to a stacking sequence basis, adding bidirectional layers as consideration of the symmetricity of laminates, and dropout to reduce overfitting of the model to training data. In this study, we incorporate the through-thickness stress distributions at varying radial distances from the hole boundary into additional channels in the LSTM network.

Convolutional neural networks (CNN) are a form of artificial neural networks that are more suited to image predictions, whereby spatial influences are important [39]. As the output in this study (stress components for each ply at multiple radial distances) is of significantly higher dimension than the input (hole geometry and laminate stacking sequence), we require the network to upsample appropriately. This is done using (transpose) convolution. The network used in this study follows a structure similar to that of a U-net decoder [40], see Fig. 2b, which is a common image processing machine learning network structure. Such a model was used in a previous study [21].

2.3. Finite element modelling

We use Abaqus/2021 to develop our implicit finite element models and run their simulations [29]. Modelling details are shown in Fig. 3. Our coupon specimens are modelled according to a successfully validated methodology [41]. We model the coupon specimen using geometry as defined by ASTM standards for open-hole tensile testing of composite laminates (ASTM D5766_D5766M-23 [42]). We vary hole

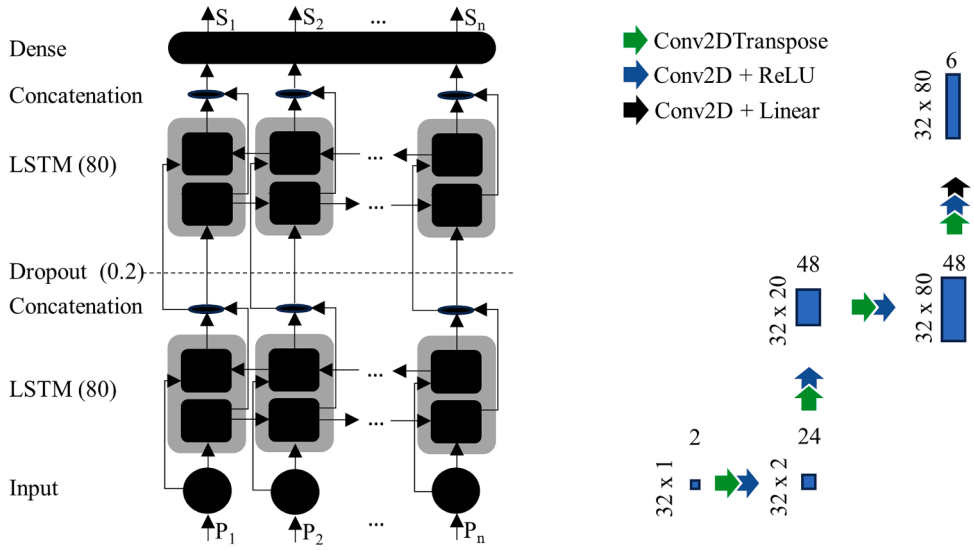

Fig. 2. Block diagrams of machine learning models used in study.

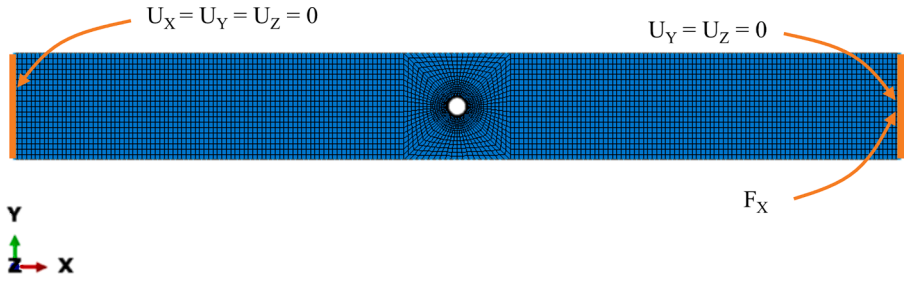

Fig. 3. FE modelling details.

diameter within a range from 2 mm to 4 mm. We use plies of 0.125 mm thickness. We limit the upper bound of laminate thickness to 4 mm, use a width to diameter ratio of 6 and a specimen length of 200 mm, as defined in the ASTM standard [42].

The elastic properties of the IM7/8552 carbon fibre composite, that is used for our linear elastic models, are defined in Table 1. In addition, the in-situ shear strength is obtained from [43] as 100 MPa. Non-linear geometry effects are turned off for our linear elastic models. For our progressive damage models, we use a Hashin failure criteria [44] with damage initiation and evolution parameters as shown in Table 2. It has been found that to successfully model the size effect of open-hole composite specimens, and reduce overprediction of failure loads, it is required to model cohesive damage [41]. Therefore, in our progressive damage models, we use thin cohesive layers with properties as defined by Table 3.

For our progressive damage coupon specimens, we model each ply using a layer of continuum shell elements (SC8R) and we model each cohesive layer with cohesive elements (COH3D). For our linear models, we use solid elements (C3D8R) with one element per ply in the thickness direction. We use a mesh size of 0.5 mm, with additional circular partitions in the vicinity of the hole boundary to improve predictions in the region of high stress concentration.

When loading our coupon specimens, we fix one end at all degrees of freedom, and we fix all degrees of freedom at the loaded end, apart from one axial degree of freedom whereby a force is applied. We apply a force rather than a displacement, as the stresses given a unit of applied force to the linear elastic model are scaled by the failure load derived from the progressive damage model.

Table 1
Material properties of IM7/8552 [41].

(GPa)	E_{22} (GPa)	E_{33} (GPa)	ν_{12}	ν_{13}	ν_{23}	G_{12} (GPa)	G_{13} (GPa)	G_{23} (GPa)
161	11.4	11.4	0.32	0.32	0.43	5.17	5.17	3.98

3. Results

3.1. Failure load prediction

We train multiple neural networks to directly predict the ultimate failure load of the open hole. This includes using Random Forest, XGBoost, Gaussian Processes and ANN. We also train a neural network to indirectly predict the ultimate failure load, by first predicting the load-displacement profile, using an ANN. Comparisons in the test accuracies for these networks, across multiple training dataset sizes, are given in Fig. 4. A violin plot showing the distribution of failure loads in the test set is also provided for reference in Fig. 4. A violin plot is similar to a box plot as it presents the median, interquartile range, maximum and minimum values. However, a violin plot additionally presents a probability density plot to show the distribution of values. In Fig. 5, we demonstrate an example prediction of failure load through direct and indirect ANN methods, using the maximum training dataset size.

3.2. Linear elastic stress field prediction

We use a LSTM neural network and a CNN to predict the linear elastic stress field of the open-hole specimens. The stress quantities of particular interest in the Yamada Sun Failure criterion, used in this work to determine failure in combination with the average stress criterion, are

Table 2
Damage initiation and evolution properties of IM7/8552 [41].

(MPa)	X_C (MPa)	Y_T (MPa)	Y_C (MPa)	S_L (MPa)	S_C (MPa)	G^c_{ft} (N/mm)	G^c_{fc} (N/mm)	G^c_{mt} (N/mm)	G^c_{mc} (N/mm)
2806	1690	60	185	90	120	112.7	112.7	0.311	0.311

Table 3
Cohesive elastic, damage initiation and evolution properties [41].

(MPa)	E_{ss} (MPa)	E_{tt} (MPa)	t_n (MPa)	t_s (MPa)	t_t (MPa)	η	G^c_n (N/mm)	G^c_s (N/mm)	G^c_t (N/mm)
4560	2068	1592	40	50	50	1.45	0.293	0.631	0.631

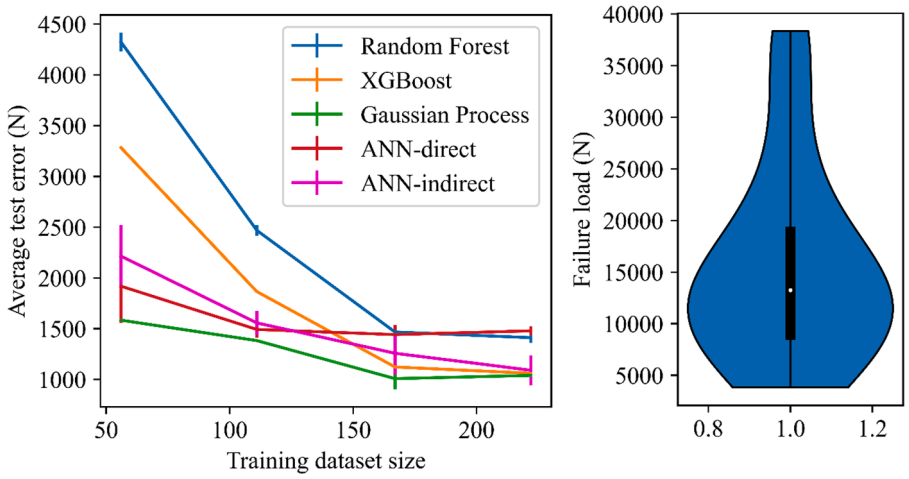

Fig. 4. Test accuracies of direct and indirect ML prediction methods for failure load (left) and violin plot of failure loads in test dataset (right).

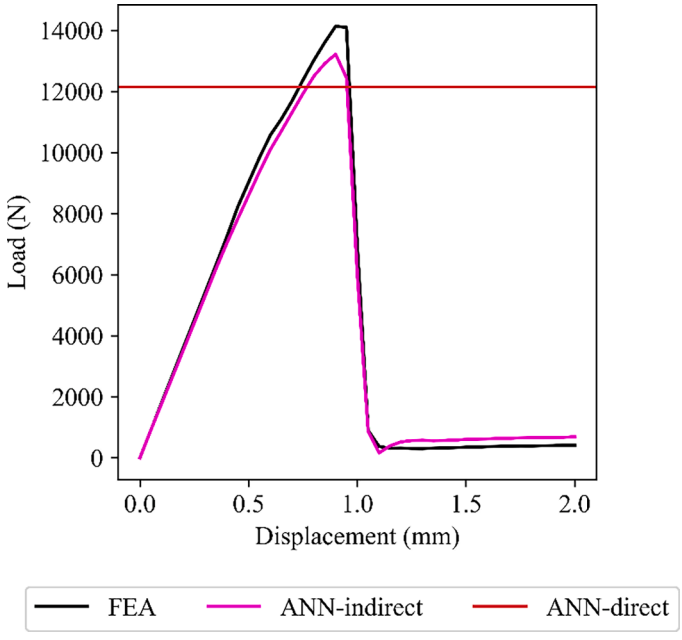

Fig. 5. Comparison of failure load predictions using direct and indirect ANN.

σ_{11} and σ_{12}. The test accuracies for the neural networks, across multiple training dataset sizes, are presented in Fig. 6. Violin plots showing the distribution of stresses in the test set are also provided for reference in Fig. 6. Example predictions of through-thickness and radial stress distributions using these neural networks, with the maximum training dataset size, are shown in Fig. 7.

3.3. Characteristic length prediction

We train multiple neural networks to directly predict the characteristic length of the open hole specimens, as determined from the failure load and linear elastic stress field in combination with the Yamada Sun Failure Index and the average stress criterion. Random Forest, XGBoost, Gaussian Processes and ANN are used for these direct predictions. We also train high-performance networks from the previous sections to indirectly predict the characteristic length. Therefore, we use an indirect-ANN method to predict failure load and a LSTM neural network to predict the linear elastic stress field. We compare the test accuracies of these direct and indirect methods, across multiple training dataset sizes, in Fig. 8. A violin plot showing the distribution of characteristic lengths in the test set is also provided for reference in Fig. 8.We present example predictions of radial stress distribution of failure index using indirect methods, at the maximum and minimum training dataset size, in Fig. 9.

Overall, the use of ML to indirectly predict failure load takes up to 115 ms CPU time, as opposed to up to 72 h using progressive damage FEA. The use of LSTM neural networks to predict linear elastic stress field takes up to 1 s CPU time, as opposed to 102 s using linear elastic FEA. Direct prediction of characteristic length takes on average 550 ms CPU time.

4. Discussions

From Fig. 4, we observe that Gaussian Process Regression offers the best direct prediction performance for failure loads across training dataset sizes. Gaussian Process Regression typically performs well for low dataset regimes, as covariance functions can provide a continuous interpolation between training samples. With increasing dataset size and dimensionality, defined covariance functions may struggle to generalise to data and result in underfitting. Accordingly, we find that direct

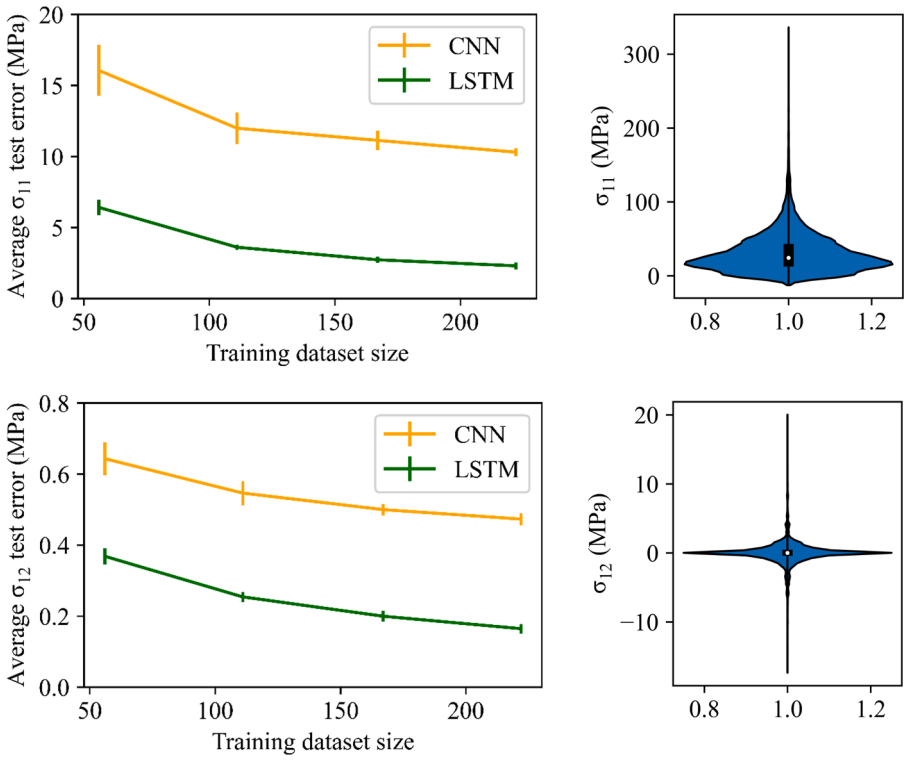

Fig. 6. Test accuracies of stress field predictions (left) and violin plot of stress components in test dataset (right).

prediction using XGBoost and indirect prediction using ANN perform as well as the Gaussian Process Regression at the maximum training dataset size investigated. These three networks may therefore be used in ensembling methods to result in improved accuracy, especially after 200 training samples.

From Fig. 4, we also see that indirect prediction using ANN results in higher errors than direct prediction using ANN for low training dataset sizes. However, the larger the training dataset size, the greater the reduction in test error using the indirect method whereas the test error using the direct method has stagnated. The indirect method requires the prediction of the entire load-displacement profile as opposed to a singular load. Due to the additional variance in the larger output feature size, it may thus be reasoned that more training data is required for the indirect model to effectively learn before error convergence. From Fig. 5, we see that the prediction of the load-displacement curve allows the model to capture the stiffness behaviour of the laminate, and therefore the maximum load prediction is more accurate than without this information, when using the same type of neural network.

In Fig. 6, the LSTM neural network method has superior performance to the CNN over all training dataset sizes, for both stress components investigated. Furthermore, we observe this superior prediction performance for an example laminate in Fig. 7, both in through-thickness and radial directions. This result indicates that the convolutional kernels used in CNNs does not provide improvements in the prediction of the stress field. Conceptually, the stress field in the net section plane is better predicted as independent parallel radial cross-sections, as opposed to an image with through thickness and radial influences. For both the CNN and LSTM, errors have not converged with the maximum training dataset size and are likely to continue reducing with further training data.

Stress distributions in the through-thickness direction are strongly related to ply angles and therefore vary significantly between plies. Conversely, stress distributions in the radial direction are continuous and vary more smoothly. The LSTM is able to accurately capture through-thickness stress distributions at a given radial distance, making benefit of bi-directionality to account for long-range effects [22]. When repeated at various radial distances the predictions made by the LSTM maintain accuracy, though such predictions are not correlated with each other resulting in slight discontinuities in the radial direction. CNNs have the potential to consider correlations in the radial direction, as they apply a convolutional kernel to patches across the image. However, the convolutional kernels used in this study (3 × 3 pixels) are of low dimensions in comparison to the image (80 × 80 pixels). Therefore, long-range effects in the radial and through-thickness directions may not be fully considered by the CNN, and short-range effects may be disproportionately valued. This may result in a counter-productive effect from the CNN that results in poor predictions in the through-thickness direction and highly discrete predictions in the radial direction.

From Fig. 8, we observe that direct prediction of characteristic length shows similar errors across ML methods. It is further observed that the models show insignificant improvements, and in some cases marginal degradation of performance, with increasing dataset size. This performance limitation from direct prediction, across hypertuned model architectures, indicates that the input-output mapping contains insufficient information for the models to further learn from. On the other hand, test errors using indirect methods show a reduction with increases in training dataset sizes, eventually outperforming direct prediction methods. As failure load prediction and linear elastic stress field prediction showed improved performance with greater training dataset size, it follows that indirect characteristic length prediction shows this same behaviour. For larger dataset sizes, this error is likely to reduce further, and greater outperform direct methods.

We can readily change the failure criterion used to determine the characteristic length using the indirect method, whereas we would have to retrain our direct ML model under such a change, therefore making indirect methods more flexible. Indirect prediction of characteristic length also allows us to visualise the radial variation of failure indices, see Fig. 9. This results in more interpretable (and less of a 'black box') prediction than direct predictions of the characteristic length. For example, from Fig. 9 we observe the improved prediction of failure index distribution given a greater training dataset size. However, the

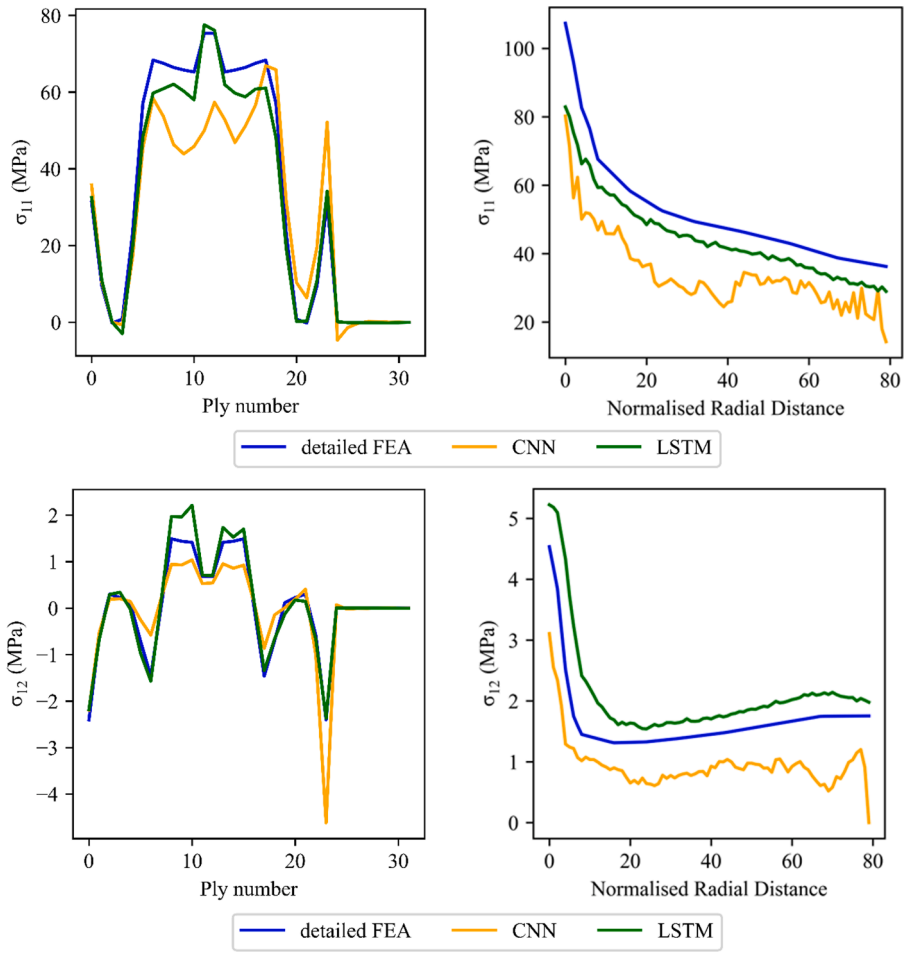

Fig. 7. Examples of through-thickness and radial predictions.

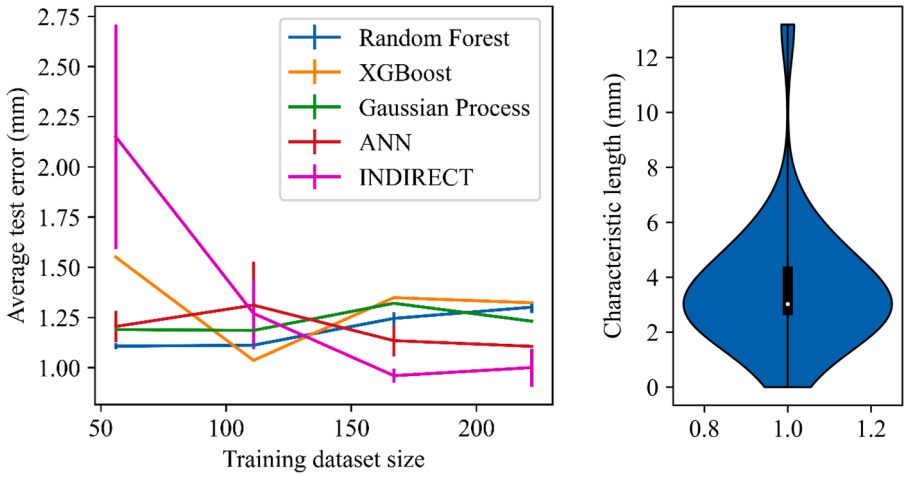

Fig. 8. Test error in characteristic length prediction (left) and violin plot of characteristic lengths in test dataset (right).

error in characteristic length prediction compounds depending on the intersection of the failure threshold (in this case equal to 1) with the failure index distribution. When this intersection occurs at a point when the radial gradient of failure index distribution is high, the error in characteristic length prediction is lower than when the intersection occurs where the radial gradient is low. That is to say, the radial gradient of the predicted failure index distributions at the failure index indicates the uncertainty in the prediction of characteristic length.

5. Conclusions

In this study, we used direct and indirect machine learning methods to predict failure load, linear elastic stress distributions and characteristic lengths as required for the average stress criterion to determine the failure of open-hole composite features.

Indirect prediction of failure load offers similar performance to the best-performing direct prediction methods, as more training samples are

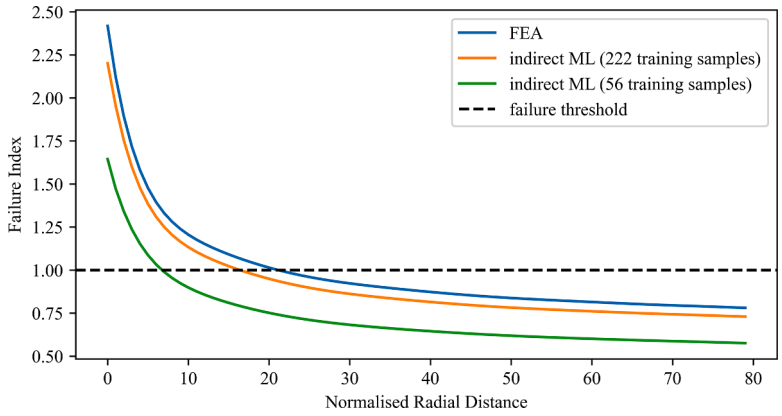

Fig. 9. Example radial distributions of failure indices using indirect ML.

generated. The load-displacement related context is shown to usefully inform maximum load prediction, as compared to without this information.

Long-short term memory neural networks predict linear elastic stress distributions in the net section plane better than convolutional neural networks. This shows that the stress field is better predicted as independent through thickness cuts at discrete radial locations, as opposed to a 2D image with spatial influences.

We show that indirect prediction of characteristic length outperforms direct prediction accuracy with increasing dataset size. Indirect prediction of characteristic length allows more customisable results as we can change the failure index criterion easily. Furthermore, indirect prediction allows more interpretable results as we can visualise the predicted failure index distribution and determine the expected uncertainty in characteristic length prediction given the radial gradient of these failure index distributions.

Our machine learning enhanced predictions of characteristic lengths result in greater than five orders of magnitude improvement in CPU time, as compared to progressive and linear elastic FEA. Such a machine learning-enhanced method can therefore be highly useful at the early design stage of large composite structures.

CRediT authorship contribution statement

Omar A.I. Azeem: Data curation, Formal analysis, Investigation, Methodology, Validation, Writing – original draft, Writing – review & editing. **Silvestre T. Pinho:** Conceptualization, Funding acquisition, Supervision, Writing – review & editing.

Declaration of competing interest

The authors declare that they have no known competing financial interests or personal relationships that could have appeared to influence the work reported in this paper.

Acknowledgments

This study was supported by funding from the Department of Aeronautics, Imperial College London. The second author acknowledges funding from EPSRC project EP/W022508/1. The authors express gratitude and remembrance of the kind support and supervision of the late Professor Lorenzo Iannucci.

Data availability

Data will be made available on request.

References

[1] C. Kassapoglou, Holes. Modeling the Effect of Damage in Composite Structures: Simplified Approaches, wiley, 2015, pp. 9–40, https://doi.org/10.1002/9781119013228.
[2] J.M. Whitney and R.J. Nuismer, 'Stress fracture criteria for laminated composites containing stress concentrations', vol. 8, no. 3, pp. 253–265, Jul. 1974, https://doi.org/10.1177/002199837400800303.
[3] HyperSizer, 'Bolted joint analyses'. (2014) Accessed: Dec. 10, 2023. [Online]. Available: https://hypersizer.com/help_7.0/Content/Failure/BJSFM/bjsfm-about.php.
[4] P.P. Camanho, M. Lambert, A design methodology for mechanically fastened joints in laminated composite materials, Compos. Sci. Technol. 66 (15) (2006) 3004–3020, https://doi.org/10.1016/J.COMPSCITECH.2006.02.017. Dec.
[5] J. Zhang, F. Liu, L. Zhao, Y. Chen, B. Fei, A progressive damage analysis based characteristic length method for multi-bolt composite joints, Compos. Struct. 108 (1) (2014) 915–923, https://doi.org/10.1016/J.COMPSTRUCT.2013.10.026. Feb.
[6] F.K. Chang, R.A. Scott, G.S. Springer, Strength of Mechanically Fastened Composite Joints, J. Compos. Mater. 16 (6) (1982) 470–494, https://doi.org/10.1177/002199838201600603.
[7] S.G. Lekhnitskii, 'Anisotropic plates', 1968. Accessed: Dec. 10, 2023. [Online]. Available: https://apps.dtic.mil/sti/citations/AD0683218.
[8] J. Koord, J.L. Stüven, O. Völkerink, E. Petersen, C. Hühne, Investigation of exact analytical solutions for composite laminates under pin-bearing loading, Compos. Struct. 292 (2022) 115605, https://doi.org/10.1016/J.COMPSTRUCT.2022.115605. Jul.
[9] J.H. Kweon, H.S. Ahn, J.H. Choi, A new method to determine the characteristic lengths of composite joints without testing, Compos. Struct. 66 (1–4) (2004) 305–315, https://doi.org/10.1016/J.COMPSTRUCT.2004.04.053. Oct.
[10] M.M. Moure, J. Herrero-Cuenca, S.K. García-Castillo, E. Barbero, Design tool to predict the open-hole failure strength of composite laminates subjected to in-plane loads, Compos. Struct. 238 (2020) 111970, https://doi.org/10.1016/J.COMPSTRUCT.2020.111970. Apr.
[11] C. Soutis, N.A. Fleck, P.A. Smith, Failure prediction technique for compression loaded carbon fibre-epoxy laminate with open holes, J. Compos. Mater. 25 (11) (1991) 1476–1498, https://doi.org/10.1177/002199839102501106. Nov.
[12] M.E. Waddoups, J.R. Eisenmann, B.E. Kaminski, Macroscopic fracture mechanics of advanced composite materials, J. Compos. Mater. 5 (4) (1971) 446–454, https://doi.org/10.1177/002199837100500402. Apr.
[13] P.P. Camanho, G.H. Erçin, G. Catalanotti, S. Mahdi, P. Linde, A finite fracture mechanics model for the prediction of the open-hole strength of composite laminates, Compos. Part A Appl. Sci. Manuf. 43 (8) (2012) 1219–1225, https://doi.org/10.1016/J.COMPOSITESA.2012.03.004. Aug.
[14] C. Furtado, A. Arteiro, M.A. Bessa, B.L. Wardle, P.P. Camanho, Prediction of size effects in open-hole laminates using only the Young's modulus, the strength, and the R-curve of the 0° ply, Compos. Part A Appl. Sci. Manuf. 101 (2017) 306–317, https://doi.org/10.1016/J.COMPOSITESA.2017.04.014. Oct.
[15] C. Furtado, et al., A methodology to generate design allowables of composite laminates using machine learning, Int. J. Solids Struct. 233 (2021) 111095, https://doi.org/10.1016/J.IJSOLSTR.2021.111095. Dec.
[16] B.A. Budiman, H. Budijanto, F. Adziman, F. Triawan, R. Wirawan, I.P. Nurprasetio, On predicting crack length and orientation in twill-woven CFRP based on limited data availability using a physics-based, high fidelity machine learning approach, Compos. Part C: Open Access 11 (2023) 100371, https://doi.org/10.1016/J.JCOMC.2023.100371. Jul.
[17] S. Suman, K. Dwivedi, S. Anand, H. Pathak, XFEM–ANN approach to predict the fatigue performance of a composite patch repaired aluminium panel, Compos. Part C: Open Access 9 (2022) 100326, https://doi.org/10.1016/J.JCOMC.2022.100326. Oct.
[18] V. Krokos, V. Bui Xuan, S.P.A. Bordas, P. Young, P. Kerfriden, A Bayesian multiscale CNN framework to predict local stress fields in structures with microscale features, Comput. Mech. 69 (3) (2022) 733–766, https://doi.org/10.1007/S00466-021-02112-3. Mar.

[19] A. Bhaduri, A. Gupta, L. Graham-Brady, Stress field prediction in fiber-reinforced composite materials using a deep learning approach, Compos. B Eng. 238 (2022) 109879, https://doi.org/10.1016/J.COMPOSITESB.2022.109879. Jun.
[20] Z. Yang, C.H. Yu, M.J. Buehler, Deep learning model to predict complex stress and strain fields in hierarchical composites, Sci. Adv. 7 (15) (2021), https://doi.org/10.1126/SCIADV.ABD7416/SUPPL_FILE/ABD7416_SM.PDF. Apr.
[21] O.A.I. Azeem, S.T. Pinho, A physics-informed machine learning model for global-local stress prediction of open holes with finite-width effects in composite structures, J. Compos. Mater. (2024), https://doi.org/10.1177/00219983241281073.
[22] O.A.I. Azeem, S.T. Pinho, A machine learning assisted multifidelity modelling methodology to predict 3D stresses in the vicinity of design features in composite structures, Int. J. Solids Struct. 301 (2024) 112946, https://doi.org/10.1016/J.IJSOLSTR.2024.112946. Sep.
[23] L. Ali, et al., Integrated behavioural analysis of FRP-confined circular columns using FEM and machine learning, Compos. Part C: Open Access 13 (2024) 100444, https://doi.org/10.1016/J.JCOMC.2024.100444. Mar.
[24] S. Ali Talpur, et al., Machine learning approach to predict the strength of concrete confined with sustainable natural FRP composites, Compos. Part C: Open Access 14 (2024) 100466, https://doi.org/10.1016/J.JCOMC.2024.100466. Jul.
[25] H.T. Fan, H. Wang, Predicting the Open-Hole Tensile Strength of Composite Plates Based on Probabilistic Neural Network, Appl. Compos. Mater. 21 (6) (2014) 827–840, https://doi.org/10.1007/S10443-014-9387-2/TABLES/7. Nov.
[26] M.K. Kazi, F. Eljack, E. Mahdi, Predictive ANN models for varying filler content for cotton fiber/PVC composites based on experimental load displacement curves, Compos. Struct. 254 (2020) 112885, https://doi.org/10.1016/J.COMPSTRUCT.2020.112885. Dec.
[27] Z. Zhang, Q. Liu, D. Wu, Predicting stress–strain curves using transfer learning: knowledge transfer across polymer composites, Mater. Des. 218 (2022) 110700, https://doi.org/10.1016/J.MATDES.2022.110700. Jun.
[28] W. Ge, V.L. Tagarielli, Data-driven constitutive models for brittle solids displaying progressive anisotropic damage, Compos. Part C: Open Access 15 (2024) 100501, https://doi.org/10.1016/J.JCOMC.2024.100501. Oct.
[29] Dassault Systemes, 'Abaqus Standard'.(2021) Accessed: Dec. 15, 2023. [Online]. Available: https://www.3ds.com/.
[30] J. Ahrens, B. Geveci, C. Law, ParaView: An End-User Tool for Large Data Visualization, Elsevier, 2005.
[31] M. Abadi et al., 'TensorFlow: a system for large-scale machine learning TensorFlow: a system for large-scale machine learning', 2016.
[32] F. Chollet, 'Keras'. (2015) Accessed: Dec. 15, 2023. [Online]. Available: https://keras.io.
[33] L. Breiman, Random forests, Mach Learn 45 (1) (2001) 5–32, https://doi.org/10.1023/A:1010933404324/METRICS. Oct.
[34] J.H. Friedman, 'Greedy function approximation: a Gradient boosting machine', vol. 29, no. 5, pp. 1189–1232, 2001.
[35] J. Görtler, R. Kehlbeck, O. Deussen, A visual exploration of gaussian processes, Distill 4 (4) (2019) e17, https://doi.org/10.23915/DISTILL.00017. Apr.
[36] D. Duvenaud, 'Kernel cookbook'. (2014) Accessed: Dec. 18, 2023. [Online]. Available: https://www.cs.toronto.edu/~duvenaud/cookbook/.
[37] Aurélien Géron, *Hands-on machine learning with Scikit-Learn, Keras and TensorFlow: concepts, tools, and techniques to build intelligent systems*. 2019.
[38] D.E. Rumelhart, G.E. Hinton, R.J. Williams, Learning representations by back-propagating errors, Nature 323 (6088) (1986) 533–536, https://doi.org/10.1038/323533a0. *1986 323:6088*.
[39] Y. Lecun, Y. Bengio, G. Hinton, Deep learning, NatureNature 521 (7553) (2015) 436–444, https://doi.org/10.1038/nature14539. *2015 521:7553*May.
[40] O. Ronneberger, P. Fischer, T. Brox, U-net: convolutional networks for biomedical image segmentation, Lecture Notes Comput. Sci. (including subseries Lecture Notes in Artif. Intell. Lecture Notes Bioinformatics) 9351 (2015) 234–241, https://doi.org/10.1007/978-3-319-24574-4_28/COVER.
[41] B.Y. Chen, T.E. Tay, P.M. Baiz, S.T. Pinho, Numerical analysis of size effects on open-hole tensile composite laminates, Compos. Part A Appl. Sci. Manuf. 47 (1) (2013) 52–62, https://doi.org/10.1016/J.COMPOSITESA.2012.12.001. Apr.
[42] ASTM, 'Standard test method for open-hole tensile strength of polymer matrix composite laminates', 2023. doi: 10.1520/D5766_D5766M-23.
[43] C. Rose, C.G. Dávila, and F.A. Leone, 'Analysis methods for progressive damage of composite structures', 2013. Accessed: Apr. 11, 2024. [Online]. Available: https://www.researchgate.net/publication/273763095_Analysis_Methods_for_Progressive_Damage_of_Composite_Structures.
[44] Z. Hashin, Failure criteria for unidirectional fiber composites, J. Appl. Mech. 47 (2) (1980) 329–334, https://doi.org/10.1115/1.3153664. Jun.